Signal Processing 93 (2013) 1349–1357

Contents lists available at SciVerse ScienceDirect

Signal Processing

journal homepage: www.elsevier.com/locate/sigpro

Maximum likelihood estimation of DOD and DOA for bistatic MIMO radar

Bo Tang [a,*], Jun Tang [b], Yu Zhang [a], Zhidong Zheng [a]

[a] Electronic Engineering Institute, Hefei 230037, Anhui Province, China
[b] Department of Electronic Engineering, Tsinghua University, Beijing 100084, China

ARTICLE INFO

Article history:
Received 24 February 2012
Received in revised form
7 November 2012
Accepted 12 November 2012
Available online 20 November 2012

Keywords:
Bistatic multiple input multiple output (MIMO) radar
Direction finding
Maximum likelihood estimation
Alternating projection

ABSTRACT

In this paper, the maximum likelihood estimation (MLE) of the direction of departure (DOD) and direction of arrival (DOA) of multiple targets for bistatic multiple input multiple output (MIMO) radar is addressed. We derive the maximum likelihood estimator of the DOD and DOA with the assumption that the targets are unknown but deterministic. Moreover, we provide a compact expression of the Cramer Rao bound (CRB) under this nonrandom framework. Since the MLE of the target DOD and DOA is related to a high-dimensional nonlinear optimization problem, we propose alternating projection (AP) to solve it efficiently. Numerical simulations demonstrate that the AP based MLE can provide accurate estimations of the target DOD and DOA and achieves the CRB in the asymptotic region. Furthermore, results also show that the proposed algorithm outperforms the existing ESPRIT and MUSIC algorithm for the uniform linear array (ULA) configuration of the transmitted and received array.

1. Introduction

Multiple input multiple output (MIMO) radar has become a hot topic which attracts great interests in recent years (see, e.g., [1–3] and the references therein). Compared with traditional phased array radar, which transmits multiple coherent waveforms, MIMO radar offers enhanced performance through waveform diversity and careful radar configurations [4–7]. Currently, MIMO radar can be classified into several types, the first of which is called statistical MIMO radar, i.e., MIMO radar with widely separated antennas. Since different aspects of the target can be viewed simultaneously by statistical MIMO radar, diversity gain and high resolution capabilities can be obtained [8,9]. The second type is the monostatic colocated MIMO radar in which the transmitters and receivers are close enough so that the direction of departure (DOD) of the target and the corresponding direction of arrival (DOA) are identical. In [5,6,10], several advantages of monostatic colocated MIMO radar, including better parameter identifiability, lower-velocity target detection and more flexible transmit beampattern design, have been demonstrated. Slightly different from monostatic colocated MIMO radar, the transmitters and receivers of bistatic MIMO radar are separated away while the transmit elements as well as receive elements are all colocated, respectively. Therefore, the DOD and DOA of a given target are distinct.

In bistatic MIMO radar, the estimation of target DOD and DOA is of much importance and has been extensively discussed recently (see, e.g., [11–17] and the references therein). In [11], a two-dimensional (2D) Capon method was used to estimate the target DOA and DOD. However, it is required to perform exhaustive 2D search to obtain high resolution angle estimations. In [12], estimation of signal parameters via rotational invariance technique (ESPRIT) was applied to the joint estimation of target DOD and DOA, in which both transmit and receive array are assumed to be uniform linear arrays (ULA). Lately, the ESPRIT algorithm proposed in [12] was further improved in [13] where the DOD and DOA are automatically paired. In [14], close form solution for DOD and DOA estimation with ESPRIT was derived, in which spatially colored noise

* Corresponding author. Tel.: +86 055165927608.
E-mail address: tangbo06@gmail.com (B. Tang).

0165-1684/$ - see front matter © 2012 Elsevier B.V. All rights reserved.
http://dx.doi.org/10.1016/j.sigpro.2012.11.011

can be canceled with three-transmitter configuration. To eliminate the limitation on the number of transmitters in [14], singular value decomposition (SVD) of the cross correlation matrix was utilized in [16]. In [15], 2D multiple signal classification (MUSIC) and a double polynomial root finding procedure are proposed for estimating the target DOD and DOA. In [17], a new method for alleviating the computation burden of 2D MUSIC method was proposed. The target DOD and DOA can be obtained by one-dimensional (1D) search. Moreover, since the method does not impose any constraint on the array configuration, it might be applied to nonuniform linear arrays.

Among these methods, most of them belong to the subspace algorithms, in which it is required the targets are uncorrelated and the signal space can be correctly split from the noise subspace. Thus we need adequate independent and identically distributed (i.i.d.) samples and enough high target signal to noise ratio (SNR) to correctly estimate the signal space. Besides, the ESPRIT-based algorithm and polynomial-root-based algorithm can only be applied to the ULA case. Compared with the subspace algorithms, it has been recognized that the maximum likelihood estimator can work with arbitrary array geometry and arbitrary number of samples. Moreover, it is asymptotically efficient, which can attain the Cramer–Rao bound (CRB) in the asymptotic region. Thus in this paper, we consider the maximum likelihood estimation (MLE) of the target DOD and DOA for bistatic MIMO radar, which has not been discussed yet, to the best of the authors' knowledge. After formulating the MLE problem of DOD and DOA, we found that the MLE is related to a high-dimensional nonlinear optimization problem, which is typically computationally prohibitive. To solve the MLE problem efficiently, we propose alternating projection (AP) technique to reduce the computation load, by which the original global search in multiple dimensions is replaced by multiple 1D optimization problems. Moreover, a method for adaptively determining the search space in the 1D global optimization is also proposed, which can accelerate the convergence and improve the estimation accuracy of the proposed algorithm.

The remainder of this paper is organized as follows. In Section 2, we present the signal model for the bistatic MIMO radar, followed by a comparison with the monostatic MIMO radar and a preliminary discussion on the localization accuracy of the bistatic MIMO radar in Section 3. Then we derive a compact expression of the CRB for the unbiased estimation of the target DOD and DOA in Section 4. In Section 5, the maximum likelihood estimator of the target DOD and DOA for the bistatic MIMO radar is derived. To solve the high-dimensional nonlinear optimization problem in the MLE efficiently, we propose the AP algorithm in Section 6. Numerical simulation is conducted in Section 7 to illustrate the performance of the proposed algorithm. Finally, we draw the conclusion in Section 8.

Notation: Throughout this paper, $\mathbb{R}$ and $\mathbb{C}$ denote the set of real and complex number. $\mathbb{R}^{m\times n}$ and $\mathbb{C}^{m\times n}$ are the sets of matrices of size $m\times n$ with entries from $\mathbb{R}$ and $\mathbb{C}$, respectively. Matrices are denoted by bold italic capital letters, and vectors are denoted by bold italic lowercase letters. Superscript $(\cdot)^T$, $(\cdot)^*$ and $(\cdot)^H$ denote transpose, conjugate, and conjugate transpose, respectively. $\det(\cdot)$ and $\mathrm{tr}(\cdot)$ represent determinant and trace of a matrix, respectively. We use $\boldsymbol{I}_M$ to denote an identity matrix of size $M\times M$. The complex Gaussian distribution with mean $\boldsymbol{m}$ and variance $\boldsymbol{\Sigma}$ is denoted by $\mathcal{CN}(\boldsymbol{m},\boldsymbol{\Sigma})$.

2. Signal model

Consider a bistatic MIMO radar with N_t transmit elements and N_r receive elements, with a system layout described in Fig. 1. For simplicity, we assume that both of them are linear arrays. Assume that N_t ideally orthogonal waveforms are transmitted and denote them by $s_1(t),\ldots,s_{N_t}(t)$, respectively. Then the signal that reaches the target can be written as

$$\boldsymbol{a}_t^T(\theta_t)\boldsymbol{S}(t), \tag{1}$$

where $\boldsymbol{a}_t(\theta_t)\in\mathbb{C}^{N_t\times 1}$ is the corresponding transmit steering vector of the target with DOD θ_t and $\boldsymbol{S}(t)=[s_1(t),\ldots,s_{N_t}(t)]^T\in\mathbb{C}^{N_t\times 1}$.

Assume P targets exist in the range bin of interest, with DOD $\theta_1,\ldots,\theta_P$ and the corresponding DOA $\phi_1,\ldots,\phi_P$, respectively. Thus the received signal can be written as

$$\boldsymbol{r}(t)=\sum_{i=1}^{P}\beta_i\boldsymbol{a}_r(\phi_i)\boldsymbol{a}_t^T(\theta_i)\boldsymbol{S}(t)+\boldsymbol{n}_1(t), \tag{2}$$

where β_i is the complex amplitude of the ith target, $\boldsymbol{a}_r(\phi_i)\in\mathbb{C}^{N_r\times 1}$ is the receive steering vector of ϕ_i and $\boldsymbol{n}_1(t)\in\mathbb{C}^{N_r\times 1}$ is the noise in the receiver.

Therefore, the output of $\boldsymbol{r}(t)$ after matched filtering and vectorization can be written as

$$\begin{aligned}\boldsymbol{y}&=\sum_{i=1}^{P}\beta_i\boldsymbol{a}_t(\theta_i)\otimes\boldsymbol{a}_r(\phi_i)+\boldsymbol{n}\\&=\boldsymbol{A}\boldsymbol{\beta}+\boldsymbol{n},\end{aligned} \tag{3}$$

where $\otimes$ denotes the Kronecker product, $\boldsymbol{n}\in\mathbb{C}^{N_tN_r\times 1}$ is the output of the noise, $\boldsymbol{A}=[\boldsymbol{a}_t(\theta_1)\otimes\boldsymbol{a}_r(\phi_1),\ldots,\boldsymbol{a}_t(\theta_P)\otimes\boldsymbol{a}_r(\phi_P)]\in\mathbb{C}^{N_tN_r\times P}$ is the transmit–receive array manifold and $\boldsymbol{\beta}=[\beta_1,\ldots,\beta_P]^T\in\mathbb{C}^{P\times 1}$.

Typically, multiple i.i.d. samples are used to estimate $\{\theta_i,\phi_i\}, i=1,\ldots,P$, and the corresponding signal model with multiple snapshots can be written as

$$\boldsymbol{y}(k)=\boldsymbol{A}\boldsymbol{\beta}(k)+\boldsymbol{n}(k),\quad k=1,\ldots,K, \tag{4}$$

where K is the number of snapshots and $\boldsymbol{y}(k)$ is the kth sample.

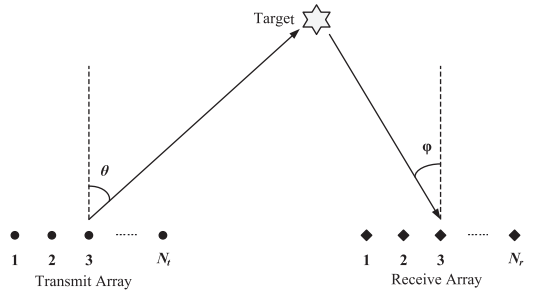

Fig. 1. System layout of the bistatic MIMO radar.

3. Performance comparisons and discussions

3.1. Comparisons with monostatic colocated MIMO radar

The monostatic colocated MIMO radar can be treated as a special case of the bistatic MIMO radar in which the target DOD and DOA are equal. Its signal model can be written as [18]

$$\boldsymbol{y}_{\mathrm{M}}(k)=\boldsymbol{A}_{\mathrm{M}}\boldsymbol{\beta}(k)+\boldsymbol{n}(k),\quad k=1,\ldots,K, \tag{5}$$

where $\boldsymbol{A}_{\mathrm{M}}=[\boldsymbol{a}_t(\theta_1)\otimes\boldsymbol{a}_r(\theta_1),\ldots,\boldsymbol{a}_t(\theta_P)\otimes\boldsymbol{a}_r(\theta_P)]\in\mathbb{C}^{N_tN_r\times P}$ is the transmit–receive array manifold of the monostatic colocated MIMO radar, θ_i is the DOA (or DOD) of the ith target.

Next we compare the performance of the monostatic MIMO radar with its bistatic counterpart. In the comparisons, unless otherwise stated, we assume they both utilize ULAs in both transmitters and receivers with the same number of array elements and transmitting orthogonal waveforms.

First, we can observe from (5) the number of unknown parameters of monostatic MIMO radar we are interested in (i.e., $\theta_1,\theta_2,\ldots,\theta_P$) equals P, which is less than the bistatic MIMO case ($2P$ in this situation). Thus we can expect the estimation accuracy of the DOA (or DOD) for the monostatic case will be higher than that of bistatic MIMO radar. On the other hand, if orthogonal waveforms are transmitted, extended array aperture can be obtained by monostatic MIMO radar. For example, for the case where the received array is a filled ULA (with half wavelength inter-element spacing) and the transmit array is a sparse array with $N_r/2$ wavelength inter-element spacing, monostatic MIMO radar can form a virtual array with N_tN_r filled elements. While for the bistatic MIMO radar, it usually uses the filled ULA as the transmitters/receivers and will lead to angle ambiguities if the transmit or receive array is sparse. Therefore, with the same number of array elements, monostatic MIMO radar can obtain higher estimation accuracy than the bistatic MIMO radar from this viewpoint.

Considering the parameter identifiability of the two cases, it is shown in [11] the maximum number of targets that can be uniquely identified by the bistatic MIMO radar can be up to N_tN_r-1. For the monostatic case, [6] showed that the maximum number of identified target varies with the array geometry, which can be much smaller than the bistatic MIMO radar if both transmit and receive array are filled ULAs.

3.2. Localization accuracy of the bistatic MIMO radar

The target localization in a bistatic MIMO radar requires (ϕ_t,R_R) from the receive array [19], where ϕ_t and R_R are the target DOA and target-to-receiver range, respectively. Typically, R_R cannot be measured directly. If the range sum (R_T+R_R) and the baseline range L (the range from the transmitter to the receiver) can be estimated, where R_T is the transmitter-to-target range, then R_R can be calculated by [19]

$$R_R=\frac{(R_T+R_R)^2-L^2}{2(R_T+R_R+L\sin\phi_t)}. \tag{6}$$

It is shown that the target-to-receiver range is a function of target DOA, range sum and baseline. We assume that these measurements are independent, i.e., the corresponding measurement errors are uncorrelated, then in this situation, the target localization accuracy of the bistatic MIMO radar is given by

$$dR_R=\left\{\left[\frac{\partial R_R}{\partial(R_T+R_R)}d(R_T+R_R)\right]^2+\left(\frac{\partial R_R}{\partial L}dL\right)^2+\left(\frac{\partial R_R}{\partial\phi_t}d\phi_t\right)^2\right\}^{1/2}, \tag{7}$$

where

$$\frac{\partial R_R}{\partial(R_T+R_R)}=\frac{(R_T+R_R)^2+L^2+2L(R_T+R_R)\sin\phi_t}{2(R_T+R_R+L\sin\phi_t)^2}, \tag{8a}$$

$$\frac{\partial R_R}{\partial L}=-\frac{[L^2+(R_T+R_R)^2]\sin\phi_t+2L(R_T+R_R)}{2(R_T+R_R+L\sin\phi_t)^2}, \tag{8b}$$

$$\frac{\partial R_R}{\partial\phi_t}=-\frac{L[(R_T+R_R)^2-L^2]\cos\phi_t}{2(R_T+R_R+L\sin\phi_t)^2}, \tag{8c}$$

$d(R_T+R_R)$, dL and $d\phi_t$ are the root mean square errors (RMSE) when measuring (R_T+R_R), L and ϕ_t, respectively. From (7), we can observe the dependence of the localization accuracy on the measurement errors of the range sum, baseline range and target DOA.

There are also some other localization techniques for the bistatic MIMO radar. For example, the "theta–theta" localization technique use the baseline range L, target DOD θ_t and DOA ϕ_t to calculate the target-to-receiver range R_R. Similarly, we can find out the dependence of the localization accuracy on the measurement accuracy of L, θ_t and ϕ_t in this circumstance (detailed derivation is omitted here). Therefore, estimating the target DOD and DOA accurately can reduce the localization errors significantly. Next we establish the Cramer Rao low bound for MSE of the unbiased estimate of the target DOD and DOA and focus on the MLE algorithm to gain the estimation result.

4. Cramer Rao bound

Before deriving the maximum likelihood estimator of the target DOD and DOA, we firstly present the CRB for the angle estimation in bistatic MIMO radar. Here we treat the target amplitudes $\boldsymbol{\beta}(k),k=1,\ldots,K$ as deterministic but unknown, and assume the noise in receiver $\boldsymbol{n}(k)$ is spatially white and complex Gaussian, with zero mean and variance σ^2. Although the CRB for bistatic MIMO radar under the deterministic but unknown framework is derived in [20], it seems that the matrices before and after the Hadamard product in [20] are not of the same size. Thus, we recalculate the CRB in this case with the same

procedure as [21], which is given by

$$\mathrm{CRB}(\boldsymbol{\Theta}) = \frac{\sigma^2}{2K}[\boldsymbol{H} \odot (\boldsymbol{R}_s^T \otimes \boldsymbol{1}_{2\times 2})]^{-1}, \tag{9}$$

where $\boldsymbol{\Theta} = [\theta_1, \phi_1, \ldots, \theta_P, \phi_P]^T \in \mathbb{R}^{2P\times 1}$, $\boldsymbol{H} = \boldsymbol{D}^H \boldsymbol{P}_{\boldsymbol{A}}^{\perp} \boldsymbol{D} \in \mathbb{C}^{2P\times 2P}$, $\boldsymbol{D} = [\boldsymbol{d}(\theta_1), \boldsymbol{d}(\phi_1), \ldots, \boldsymbol{d}(\theta_P), \boldsymbol{d}(\phi_P)] \in \mathbb{C}^{N_t N_r \times 2P}$, $\boldsymbol{d}(\theta_i) = \partial(\boldsymbol{a}_t(\theta_i) \otimes \boldsymbol{a}_r(\phi_i))/\partial(\theta_i)$, $\boldsymbol{d}(\phi_i) = \partial(\boldsymbol{a}_t(\theta_i) \otimes \boldsymbol{a}_r(\phi_i))/\partial(\phi_i)$, $\boldsymbol{P}_{\boldsymbol{A}}^{\perp} = \boldsymbol{I} - \boldsymbol{P}_{\boldsymbol{A}}$, $\boldsymbol{P}_{\boldsymbol{A}} = \boldsymbol{A}(\boldsymbol{A}^H\boldsymbol{A})^{-1}\boldsymbol{A}^H$, $\odot$ denotes the Hadamard product, $\boldsymbol{R}_s = 1/K \sum_{k=1}^{K} \boldsymbol{\beta}(k)\boldsymbol{\beta}^H(k) \in \mathbb{C}^{P\times P}$ and $\boldsymbol{1}_{2\times 2}$ is a 2×2 matrix filled with ones.

For the joint DOD and DOA estimate of a single target with the bistatic MIMO radar, the corresponding CRB for estimating $\psi_t = \pi \sin\theta_1$ and $\psi_r = \pi \sin\phi_1$ is given by

$$\mathrm{CRB}(\psi_t, \psi_r) = \frac{1}{2K\widehat{\mathrm{SNR}}} \begin{bmatrix} (\|\boldsymbol{d}_t\|^2/N_t - |\boldsymbol{a}_t^H\boldsymbol{d}_t|^2/N_t^2)^{-1} & 0 \\ 0 & (\|\boldsymbol{d}_r\|^2/N_r - |\boldsymbol{a}_r^H\boldsymbol{d}_r|^2/N_r^2)^{-1} \end{bmatrix}, \tag{10}$$

where $\widehat{\mathrm{SNR}} = N_t N_r \sum_{k=1}^{K} |\beta(k)|^2/(K\sigma^2)$ is the average SNR, $\boldsymbol{d}_t = \partial \boldsymbol{a}_t(\psi_t)/\partial\psi_t$ and $\boldsymbol{d}_r = \partial \boldsymbol{a}_r(\psi_r)/\partial\psi_r$ (here we omit the dependence of $\boldsymbol{d}_t/\boldsymbol{d}_r$ on ψ_t/ψ_r for brevity).

If both the transmit and receive array are conjugate symmetric filled ULA [21], then $\boldsymbol{a}_t^H\boldsymbol{d}_t = 0$, $\boldsymbol{a}_r^H\boldsymbol{d}_r = 0$, and

$$\mathrm{CRB}(\psi_t, \psi_r) = \frac{1}{2K\widehat{\mathrm{SNR}}} \begin{bmatrix} 6/(N_t^2-1) & 0 \\ 0 & 6/(N_r^2-1) \end{bmatrix}. \tag{11}$$

We can observe from (11) that the variance bounds decrease with increasing number of samples, average SNR and the number of array elements. Besides, if the number of elements in the receive array is more than that in the transmit array, the estimate result of the target DOA will be more accurate than that of DOD. Moreover, we can also find out the number of elements in the transmitters impacts the variance of measurement error of the DOD more than that in receivers, since the variance bound of DOD is given by $6/[2K \cdot \sum_{k=1}^{K} |\beta(k)|^2/(K\sigma^2) \cdot N_t N_r(N_t^2-1)]$ and approximately proportional to $1/N_t^3$ while proportional to $1/N_r$. Similar conclusions also hold for that of DOA.

Now we perform the MLE of $\{\theta_i, \phi_i\}, i = 1, \ldots, P$ with $\boldsymbol{y}(k), k = 1, \ldots, K$.

5. Maximum likelihood estimation of DOD and DOA

Since the target amplitudes $\boldsymbol{\beta}(k)$ are unknown and deterministic, and $\boldsymbol{n}(k)$ are white Gaussian noise, we have $\boldsymbol{y}(k) \sim \mathcal{CN}(\boldsymbol{A}\boldsymbol{\beta}(k), \sigma^2\boldsymbol{I})$, and the joint distribution of $\boldsymbol{y}(1), \ldots, \boldsymbol{y}(K)$ is given by

$$p(Y) = \prod_{k=1}^{K} \frac{1}{\pi^{N_t N_r} \det(\sigma^2 \boldsymbol{I})} \exp\left[-\frac{1}{\sigma^2}(\boldsymbol{y}(k) - \boldsymbol{A}\boldsymbol{\beta}(k))^H(\boldsymbol{y}(k) - \boldsymbol{A}\boldsymbol{\beta}(k))\right]. \tag{12}$$

Ignoring constant terms, the logarithm likelihood function of $\boldsymbol{y}(1), \ldots, \boldsymbol{y}(K)$ is given by

$$L(\boldsymbol{\theta}, \boldsymbol{\phi}, \boldsymbol{\beta}, \sigma^2) = -N_t N_r K \log\sigma^2 - \frac{1}{\sigma^2}\sum_{k=1}^{K}(\boldsymbol{y}(k) - \boldsymbol{A}\boldsymbol{\beta}(k))^H(\boldsymbol{y}(k) - \boldsymbol{A}\boldsymbol{\beta}(k)). \tag{13}$$

Differentiating (13) with respect to σ^2 and setting it equal zero, we can obtain the MLE of σ^2

$$\hat{\sigma}^2_{\mathrm{ML}} = \frac{1}{N_t N_r K}\sum_{k=1}^{K}(\boldsymbol{y}(k) - \boldsymbol{A}\boldsymbol{\beta}(k))^H(\boldsymbol{y}(k) - \boldsymbol{A}\boldsymbol{\beta}(k)). \tag{14}$$

Substituting (14) into (13) and ignoring constant terms, the equivalent likelihood function can be written as

$$L_2(\boldsymbol{\theta}, \boldsymbol{\phi}, \boldsymbol{\beta}) = \sum_{k=1}^{K}(\boldsymbol{y}(k) - \boldsymbol{A}\boldsymbol{\beta}(k))^H(\boldsymbol{y}(k) - \boldsymbol{A}\boldsymbol{\beta}(k)), \tag{15}$$

and the maximization of $L(\boldsymbol{\theta}, \boldsymbol{\phi}, \boldsymbol{\beta}, \sigma^2)$ is equivalent to the minimization of $L_2(\boldsymbol{\theta}, \boldsymbol{\phi}, \boldsymbol{\beta})$. Next we find the MLE of $\boldsymbol{\beta}(k)$. Differentiating (15) with respect to $\boldsymbol{\beta}(k)$ and setting it to zero, we have

$$\hat{\boldsymbol{\beta}}_{\mathrm{ML}}(k) = (\boldsymbol{A}^H\boldsymbol{A})^{-1}\boldsymbol{A}^H\boldsymbol{y}(k), \tag{16}$$

where $\hat{\boldsymbol{\beta}}_{\mathrm{ML}}(k)$ is the MLE of $\boldsymbol{\beta}(k)$.

Substituting (16) into (15), then we have

$$L_3(\boldsymbol{\theta}, \boldsymbol{\phi}) = \sum_{k=1}^{K} \boldsymbol{y}^H(k)\boldsymbol{P}_{\boldsymbol{A}}^{\perp}\boldsymbol{y}(k), \tag{17}$$

where we have used the matrix equality $\boldsymbol{P}_{\boldsymbol{A}}^{\perp}\boldsymbol{P}_{\boldsymbol{A}}^{\perp} = \boldsymbol{P}_{\boldsymbol{A}}^{\perp}$.

Noting that $\mathrm{tr}(\boldsymbol{AB}) = \mathrm{tr}(\boldsymbol{BA})$, we have

$$\begin{aligned} \frac{1}{K}\sum_{k=1}^{K} \boldsymbol{y}^H(k)\boldsymbol{P}_{\boldsymbol{A}}^{\perp}\boldsymbol{y}(k) &= \frac{1}{K}\sum_{k=1}^{K} \mathrm{tr}[\boldsymbol{y}^H(k)\boldsymbol{P}_{\boldsymbol{A}}^{\perp}\boldsymbol{y}(k)] \\ &= \mathrm{tr}\left[\boldsymbol{P}_{\boldsymbol{A}}^{\perp}\frac{1}{K}\sum_{k=1}^{K}\boldsymbol{y}(k)\boldsymbol{y}^H(k)\right] = \mathrm{tr}[\boldsymbol{P}_{\boldsymbol{A}}^{\perp}\boldsymbol{C}_{\boldsymbol{y}}] = \mathrm{tr}[\boldsymbol{C}_{\boldsymbol{y}}] - \mathrm{tr}[\boldsymbol{P}_{\boldsymbol{A}}\boldsymbol{C}_{\boldsymbol{y}}], \end{aligned} \tag{18}$$

where $\boldsymbol{C}_{\boldsymbol{y}} = (1/K)\sum_{k=1}^{K}\boldsymbol{y}(k)\boldsymbol{y}^H(k)$ is the sample covariance matrix (SCM).

Therefore, the MLE of $\{\theta_i, \phi_i\}, i = 1, \ldots, P$ is given by

$$\{\hat{\boldsymbol{\theta}}_{\mathrm{ML}}, \hat{\boldsymbol{\phi}}_{\mathrm{ML}}\} = \arg\max_{\boldsymbol{\theta},\boldsymbol{\phi}} \mathrm{tr}[\boldsymbol{P}_{\boldsymbol{A}}\boldsymbol{C}_{\boldsymbol{y}}]. \tag{19}$$

If $P = 1$, then $\boldsymbol{P}_{\boldsymbol{A}} = \boldsymbol{a}(\theta,\phi)\boldsymbol{a}^H(\theta,\phi)/\|\boldsymbol{a}(\theta,\phi)\|^2$, where $\boldsymbol{a}(\theta,\phi) = \boldsymbol{a}_t(\theta) \otimes \boldsymbol{a}_r(\phi)$ and

$$\{\hat{\theta}_{\mathrm{ML}}, \hat{\phi}_{\mathrm{ML}}\} = \arg\max_{\theta,\phi} \|\boldsymbol{a}(\theta,\phi)\boldsymbol{Y}\|^2, \tag{20}$$

where $\boldsymbol{Y} = [\boldsymbol{y}(1), \ldots, \boldsymbol{y}(K)]$ is the sample matrix. Therefore, the maximum likelihood estimator of the DOD and DOA for a single target is equivalent to the 2D beamformer.

While if $P > 1$, we can observe from (19) that to obtain the maximum likelihood estimation of $\{\theta_i, \phi_i\}, i = 1, \ldots, P$, we have to solve a multidimensional nonlinear optimization problem. Specifically, the number of the unknown parameters we have to estimate is $2P$, thus we have to perform a global search in a $2P$-dimensional space, which is computationally expensive. To alleviate the computation burden of the MLE of DOD and DOA, we propose alternating projection (AP) algorithm to find the estimation result in the next section.

6. Alternating projection algorithm for MLE of DOD and DOA

AP algorithm, also called by cyclic optimization elsewhere [22], refers to a type of iterative algorithm which can obtain better solutions in a sequence of successive

iterations. AP algorithm can guarantee that a local optimal solution can be found. If the objective function is non-convex, then a good initial point is necessary to find the global optimal solution. For more introductions to AP algorithm, see [23] for a reference. Now we focus on the MLE of DOD and DOA with AP algorithm.

The application of AP algorithm to parameter estimation in array signal processing is firstly presented in [24]. Here we consider the MLE for the bistatic MIMO radar with AP algorithm where the DOD and DOA of the targets should be estimated simultaneously.

A complete procedure of AP algorithm typically consists of finding a good initial point and successive iterations with updating DOD and DOA until convergence. In the MLE problem, there are many methods to obtain the initial point, e.g., [25] suggests finding the initial point by genetic algorithm (GA). In addition, if we have some *a priori* knowledge about the target or the array configuration, we can also use some other methods for the initialization of the target DOD and DOA. For example, for the uncorrelated targets, we can exploit two 1D MUSIC algorithms with pairing for finding the initial point. Here our algorithm is initialized by

$$\{\hat{\theta}_1^{(0)},\hat{\phi}_1^{(0)}\}=\arg\max_{\theta,\phi}\{\boldsymbol{P}_{\boldsymbol{a}(\theta,\phi)}\boldsymbol{C}_{\boldsymbol{y}}\} \tag{21}$$

and

$$\{\hat{\theta}_k^{(0)},\hat{\phi}_k^{(0)}\}=\arg\max_{\theta,\phi}\left\{\boldsymbol{P}_{[\boldsymbol{a}(\theta,\phi)\ \boldsymbol{A}(\hat{\boldsymbol{\theta}}^{(k-1,0)},\hat{\boldsymbol{\phi}}^{(k-1,0)})]}\boldsymbol{C}_{\boldsymbol{y}}\right\},\quad k=2,\ldots,P, \tag{22}$$

where $\hat{\theta}_k^{(0)}$ and $\hat{\phi}_k^{(0)}$ denote the estimated DOD and DOA of the kth target during the initializations, respectively, $\boldsymbol{A}(\hat{\boldsymbol{\theta}}^{(k-1,0)},\hat{\boldsymbol{\phi}}^{(k-1,0)})=[\boldsymbol{a}(\hat{\theta}_1^{(0)},\hat{\phi}_1^{(0)}),\ldots,\boldsymbol{a}(\hat{\theta}_{(k-1)}^{(0)},\hat{\phi}_{(k-1)}^{(0)})]\in\mathbb{C}^{N_tN_r\times(k-1)}$.

We can observe from (22) although $\boldsymbol{A}(\hat{\boldsymbol{\theta}}^{(k-1,0)},\hat{\boldsymbol{\phi}}^{(k-1,0)})$ is fixed, we need to recalculate $\boldsymbol{P}_{[\boldsymbol{a}(\theta,\phi)\ \boldsymbol{A}(\hat{\boldsymbol{\theta}}^{(k-1,0)},\hat{\boldsymbol{\phi}}^{(k-1,0)})]}$ for every new pair of $\{\theta,\phi\}$ due to that a new column $\boldsymbol{a}(\theta,\phi)$ is added, which increases the computation complexity. Thus the following matrix equality is employed to reduce the computation load:

Lemma 1 (*Ziskind and Wax [24]*). *For matrices* $\boldsymbol{A}\in\mathbb{C}^{M\times N_1}$ *and* $\boldsymbol{B}\in\mathbb{C}^{M\times N_2}$, *which are both column full rank, we have*

$$\boldsymbol{P}_{[\boldsymbol{A}\ \boldsymbol{B}]}=\boldsymbol{P}_{\boldsymbol{A}}+\boldsymbol{P}_{\boldsymbol{B}(\boldsymbol{A})}, \tag{23}$$

where $\boldsymbol{B}(\boldsymbol{A})=\boldsymbol{P}_{\boldsymbol{A}}^{\perp}\boldsymbol{B}$.

According to Lemma 1, we have

$$\boldsymbol{P}_{[\boldsymbol{a}(\theta,\phi)\ \boldsymbol{A}(\hat{\boldsymbol{\theta}}^{(k-1,0)},\hat{\boldsymbol{\phi}}^{(k-1,0)})]}=\boldsymbol{P}_{\boldsymbol{A}(\hat{\boldsymbol{\theta}}^{(k-1,0)},\hat{\boldsymbol{\phi}}^{(k-1,0)})}+\boldsymbol{P}_{\boldsymbol{a}(\theta,\phi)(\boldsymbol{A}(\hat{\boldsymbol{\theta}}^{(k-1,0)},\hat{\boldsymbol{\phi}}^{(k-1,0)}))} \tag{24}$$

and

$$\{\hat{\theta}_k^{(0)},\hat{\phi}_k^{(0)}\}=\arg\max_{\theta,\phi}\{[\boldsymbol{P}_{\boldsymbol{A}(\hat{\boldsymbol{\theta}}^{(k-1,0)},\hat{\boldsymbol{\phi}}^{(k-1,0)})}+\boldsymbol{P}_{\boldsymbol{a}(\theta,\phi)(\boldsymbol{A}(\hat{\boldsymbol{\theta}}^{(k-1,0)},\hat{\boldsymbol{\phi}}^{(k-1,0)}))}]\boldsymbol{C}_{\boldsymbol{y}}\}$$
$$=\arg\max_{\theta,\phi}\{\boldsymbol{P}_{\boldsymbol{a}(\theta,\phi)(\boldsymbol{A}(\hat{\boldsymbol{\theta}}^{(k-1,0)},\hat{\boldsymbol{\phi}}^{(k-1,0)}))}\boldsymbol{C}_{\boldsymbol{y}}\},\quad k=2,\ldots,P. \tag{25}$$

Therefore, we only need to calculate $\boldsymbol{P}_{\boldsymbol{a}(\theta,\phi)(\boldsymbol{A}(\hat{\boldsymbol{\theta}}^{(k-1,0)},\hat{\boldsymbol{\phi}}^{(k-1,0)}))}$ without updating the projection of a matrix with size $N_tN_r\times k$ for every new pair of $\{\theta,\phi\}$. Noting that $\boldsymbol{a}(\theta,\phi)(\boldsymbol{A}(\hat{\boldsymbol{\theta}}^{(k-1,0)},\hat{\boldsymbol{\phi}}^{(k-1,0)}))$ is a vector with length N_tN_r which can be obtained by multiplying $\boldsymbol{P}^{\perp}_{\boldsymbol{A}(\hat{\boldsymbol{\theta}}^{(k-1,0)},\hat{\boldsymbol{\phi}}^{(k-1,0)})}$ (it is fixed in every cycle) with $\boldsymbol{a}(\theta,\phi)$, we have

$$\boldsymbol{P}_{\boldsymbol{a}(\theta,\phi)(\boldsymbol{A}(\hat{\boldsymbol{\theta}}^{(k-1,0)},\hat{\boldsymbol{\phi}}^{(k-1,0)}))}=\frac{\boldsymbol{a}(\theta,\phi)(\boldsymbol{A}(\hat{\boldsymbol{\theta}}^{(k-1,0)},\hat{\boldsymbol{\phi}}^{(k-1,0)}))\boldsymbol{a}^H(\theta,\phi)(\boldsymbol{A}(\hat{\boldsymbol{\theta}}^{(k-1,0)},\hat{\boldsymbol{\phi}}^{(k-1,0)}))}{\|\boldsymbol{a}(\theta,\phi)(\boldsymbol{A}(\hat{\boldsymbol{\theta}}^{(k-1,0)},\hat{\boldsymbol{\phi}}^{(k-1,0)}))\|^2} \tag{26}$$

and

$$\{\hat{\theta}_k^{(0)},\hat{\phi}_k^{(0)}\}=\arg\max_{\theta,\phi}\{\boldsymbol{b}_{\mathrm{ini}}(\theta,\hat{\boldsymbol{\theta}}^{(k-1,0)},\phi,\hat{\boldsymbol{\phi}}^{(k-1,0)})\boldsymbol{C}_{\boldsymbol{y}}\boldsymbol{b}_{\mathrm{ini}}^H(\theta,\hat{\boldsymbol{\theta}}^{(k-1,0)},\phi,\hat{\boldsymbol{\phi}}^{(k-1,0)})\},\quad k=2,\ldots,P, \tag{27}$$

where $\boldsymbol{b}_{\mathrm{ini}}(\theta,\hat{\boldsymbol{\theta}}^{(k-1,0)},\phi,\hat{\boldsymbol{\phi}}^{(k-1,0)})=\boldsymbol{a}(\theta,\phi)(\boldsymbol{A}(\hat{\boldsymbol{\theta}}^{(k-1,0)},\hat{\boldsymbol{\phi}}^{(k-1,0)}))/\|\boldsymbol{a}(\theta,\phi)\ (\boldsymbol{A}(\hat{\boldsymbol{\theta}}^{(k-1,0)},\hat{\boldsymbol{\phi}}^{(k-1,0)}))\|$. Replacing (22) with (27), we can significantly reduce the computation load.

Note that we need search in a 2D space to find an initial point of the AP algorithm in this paper, which is a little computationally expensive. However, we do not require extremely accurate estimation of the DOD and DOA in the initialization, thus we can perform a very coarse search to find the initial point, which will save the computation costs.

In the kth iteration of the AP algorithm, we have to update the DOD and DOA of the targets, respectively. As we have explained, the total number of parameters we need to update equals $2P$. In the AP algorithm proposed by [24], the DOA of the P targets is updated sequentially in P cycles. Nevertheless, following [24], for the pth cycle in the kth iteration of the AP algorithm, we should update both target DOD and DOA, which needs a 2D global search. To further reduce the computation load, we propose firstly updating the DOD of the pth target and then the corresponding DOA in the pth cycle. Thus through breaking the original MLE into many smaller problems, we only need to perform 1D search sequentially in our AP algorithm. More specifically, for the pth cycle in the kth iteration, the DOD of the target is updated by

$$\theta_p^{(k)}=\arg\max_{\theta}\mathrm{tr}[\boldsymbol{P}_{[\boldsymbol{a}(\theta,\phi_p^{(k-1)})\ \boldsymbol{A}(\boldsymbol{\theta}_{(p)}^{(k-1)},\boldsymbol{\phi}_{(p)}^{(k-1)})]}\boldsymbol{C}_{\boldsymbol{y}}], \tag{28}$$

where $\theta_p^{(k-1)}$ and $\phi_p^{(k-1)}$ are the DOD and DOA of the pth target at the $(k-1)$ th iteration, respectively, $\boldsymbol{\theta}_{(p)}^{(k-1)}=[\theta_1^{(k)},\ldots,\theta_{p-1}^{(k)},\theta_{p+1}^{(k-1)},\ldots,\theta_P^{(k-1)}]\in\mathbb{R}^{(P-1)\times1}$, $\boldsymbol{\phi}_{(p)}^{(k-1)}=[\phi_1^{(k)},\ldots,\phi_{p-1}^{(k)},\phi_{p+1}^{(k-1)},\ldots,\phi_P^{(k-1)}]\in\mathbb{R}^{(P-1)\times1}$, which are the DOD and DOA currently obtained excluding θ_p and ϕ_p, respectively,

$$\boldsymbol{A}(\boldsymbol{\theta}_{(p)}^{(k-1)},\boldsymbol{\phi}_{(p)}^{(k-1)})=[\boldsymbol{a}(\theta_1^{(k)},\phi_1^{(k)}),\ldots,\boldsymbol{a}(\theta_{p-1}^{(k)},\phi_{p-1}^{(k)}),\boldsymbol{a}(\theta_{p+1}^{(k-1)},\phi_{p+1}^{(k-1)}),\ldots,\boldsymbol{a}(\theta_P^{(k-1)},\phi_P^{(k-1)})]\in\mathbb{C}^{N_tN_r\times(P-1)}.$$

According to Lemma 1, the update of DOD of the pth target in (28) can be simplified by

$$\theta_p^{(k)}=\arg\max_{\theta}\mathrm{tr}[\boldsymbol{b}_{\mathrm{iter}}(\theta,\boldsymbol{\theta}_{(p)}^{(k-1)},\phi_p^{(k-1)},\boldsymbol{\phi}_{(p)}^{(k-1)})\boldsymbol{C}_{\boldsymbol{y}}\boldsymbol{b}_{\mathrm{iter}}^H(\theta,\boldsymbol{\theta}_{(p)}^{(k-1)},$$

Table 1
Summary of the AP based MLE algorithm.

Step 1:	$k=0$, initialize the target DOD and DOA with (21) and (27), then we can obtain $\theta_1^{(0)},\phi_1^{(0)},\ldots,\theta_P^{(0)},\phi_P^{(0)}$.
Step 2:	$k=k+1$. For $p=1,\ldots,P$, we sequentially update $\theta_p^{(k)}$ and $\phi_p^{(k)}$ with (29) and (30).
Step 3:	If $\theta_i^{(k)},\phi_i^{(k)},i=1,\ldots,P$ satisfies (32) and (33), respectively, then stop; else return to Step 2.

$$\phi_p^{(k-1)},\boldsymbol{\phi}_{(p)}^{(k-1)})], \tag{29}$$

where $\boldsymbol{b}_{\text{iter}}(\theta,\boldsymbol{\theta}_{(p)}^{(k-1)},\phi_p^{(k-1)},\boldsymbol{\phi}_{(p)}^{(k-1)})=\boldsymbol{a}(\theta,\phi_p^{(k-1)})\quad(\boldsymbol{A}(\boldsymbol{\theta}_{(p)}^{(k-1)},\boldsymbol{\phi}_{(p)}^{(k-1)}))/\|\boldsymbol{a}(\theta,\phi_p^{(k-1)})(\boldsymbol{A}(\boldsymbol{\theta}_{(p)}^{(k-1)},\boldsymbol{\phi}_{(p)}^{(k-1)}))\|$.

After updating of DOD of the pth target in the pth cycle, the corresponding DOA can be updated as follows:

$$\phi_p^{(k)}=\arg\max_{\phi}\operatorname{tr}[\boldsymbol{b}_{\text{iter}}(\theta_p^{(k)},\boldsymbol{\theta}_{(p)}^{(k-1)},\phi,\boldsymbol{\phi}_{(p)}^{(k-1)})\boldsymbol{C}_{\boldsymbol{y}}\boldsymbol{b}_{\text{iter}}^H(\theta_p^{(k)},\boldsymbol{\theta}_{(p)}^{(k-1)},\phi,\boldsymbol{\phi}_{(p)}^{(k-1)})], \tag{30}$$

where $\boldsymbol{b}_{\text{iter}}(\theta_p^{(k)},\boldsymbol{\theta}_{(p)}^{(k-1)},\phi,\boldsymbol{\phi}_{(p)}^{(k-1)})=\boldsymbol{a}(\theta_p^{(k)},\phi)(\boldsymbol{A}(\boldsymbol{\theta}_{(p)}^{(k-1)},\boldsymbol{\phi}_{(p)}^{(k-1)}))/\|\boldsymbol{a}(\theta_p^{(k)},\phi)(\boldsymbol{A}(\boldsymbol{\theta}_{(p)}^{(k-1)},\boldsymbol{\phi}_{(p)}^{(k-1)}))\|$.

By (28) and (30), we have

$$\operatorname{tr}[\boldsymbol{P}_{[\boldsymbol{a}(\theta_p^{(k-1)},\phi_p^{(k-1)})\boldsymbol{A}(\boldsymbol{\theta}_{(p)}^{(k-1)},\boldsymbol{\phi}_{(p)}^{(k-1)})]}\boldsymbol{C}_{\boldsymbol{y}}]\le\operatorname{tr}[\boldsymbol{P}_{[\boldsymbol{a}(\theta_p^{(k)},\phi_p^{(k-1)})\boldsymbol{A}(\boldsymbol{\theta}_{(p)}^{(k-1)},\boldsymbol{\phi}_{(p)}^{(k-1)})]}\boldsymbol{C}_{\boldsymbol{y}}]$$
$$\le\operatorname{tr}[\boldsymbol{P}_{[\boldsymbol{a}(\theta_p^{(k)},\phi_p^{(k)})\boldsymbol{A}(\boldsymbol{\theta}_{(p)}^{(k-1)},\boldsymbol{\phi}_{(p)}^{(k-1)})]}\boldsymbol{C}_{\boldsymbol{y}}]. \tag{31}$$

Thus, the object function in (19) is nondecreasing in the iterations, and our AP algorithm can converge to a local maximum of the object function.

Our AP algorithm stops

$$|\theta_i^{(k)}-\theta_i^{(k-1)}|\le\varepsilon \tag{32}$$

and

$$|\phi_i^{(k)}-\phi_i^{(k-1)}|\le\varepsilon \tag{33}$$

for $\forall 1\le i\le P$, where ε is a pre-specified threshold (e.g., 1×10^{-8}).

Finally, the AP based MLE of the target DOD and DOA is summarized in Table 1.

6.1. Adapted space searching

In the proposed AP algorithm, the original MLE problem which needs a global search in a $2P$-dimensional space, now has been broken into many 1D global search problems. However, we should have noted that to obtain an extremely accurate estimate for the target DOD or DOA in the high-SNR region or the asymptotic region with infinite samples, the step size in the 1D search space should be small enough, which may increase the computation burden. To overcome this problem, note that our AP algorithm can converge to a global maximum if the initial point is good enough, which means the estimation results of the DOD and DOA become more accurate during the iterations. Based on this idea, here we propose an adapted space searching method [25] to refine the estimation result and accelerate the AP algorithm.

Let $\Theta_i^{(k)}=[a_i^{(k)},b_i^{(k)}]$ be the searching space in the kth iteration for $\theta_i^{(k)}$. The adapted searching space for $\theta_i^{(k)}$ (the adapted searching space for ϕ_i is similarly defined; however, for notation simplicity, it is omitted here) is given by

if $k<3$

$$\Theta_i^{(k)}=\Theta_i^{(0)}=[a_i^{(0)},b_i^{(0)}],$$

where $a_i^{(0)}=-\pi/2$ and $b_i^{(0)}=\pi/2$,

else calculate the gratitude for θ_i

$$\Delta_i^{(k-1)}=\theta_i^{(k-1)}-\theta_i^{(k-2)},$$
$$\Delta_i^{(k-2)}=\theta_i^{(k-2)}-\theta_i^{(k-3)};$$

if $|\Delta_i^{(k-1)}|>|\Delta_i^{(k-2)}|$,

$$a_i^{(k)}=a^{(0)},\quad b_i^{(k)}=b^{(0)},$$

else

$$a_i^{(k)}=\theta_i^{(k-1)}-w\Delta_i^{(k-1)},$$
$$b_i^{(k)}=\theta_i^{(k-1)}+w\Delta_i^{(k-1)},$$

where $w>1$ is a constant.

Through adapting the search space during the iterations in the AP algorithm while keeping the number of the searching grids invariant, we find that we can obtain highly accurate estimations of the DOD and DOA in the high SNR region.

6.2. Computational complexity analysis

In the initialization of AP algorithm, we need to perform a coarse 2D search in the region of θ and ϕ sequentially in P cycles. In the kth cycle, the algorithm requires $O(N_t^2\ N_r^2(k+k_{ct}k_{cr}))$ flops, where the first term is the cost of calculating $\boldsymbol{b}_{\text{ini}}(\theta,\hat{\boldsymbol{\theta}}^{(k-1,0)},\phi,\hat{\boldsymbol{\phi}}^{(k-1,0)})$, the second term denotes the cost in finding the maximum, k_{ct} and k_{cr} are the number of coarse search grids in the region of DOD and DOA, respectively. Thus the complexity of the proposed initialization is $O(N_t^2N_r^2(P^2/2+\ Pk_{ct}k_{cr}+K))$, where $O(N_t^2N_r^2K)$ represents the cost for computing SCM $\boldsymbol{C}_{\boldsymbol{y}}$. While in every cycle in each iteration, the computation cost is $O(N_t^2N_r^2(P\ +k_f))$, where k_f is the number of fine search grids in the region of θ and ϕ. Therefore, we need $O(2N_t^2N_r^2P(P+k_f))$ operations in every update of the target DOD and DOA. Summing up the above results, the total cost of the AP based MLE algorithm is about $O\{N_t^2N_r^2[(P^2/2+Pk_{ct}k_{cr}+K)+N_{iter}(2P^2+2Pk_f)]\}$ flops, where N_{iter} denotes the number of terations.

In contrast with the AP based MLE, the ESPRIT algorithm requires $O(N_t^2N_r^2K+N_t^3N_r^3+P^3)$ operations and the 2D MUSIC algorithm needs $O(N_t^2N_r^2K+N_t^3N_r^3+k_{mt}k_{mr}N_t^2N_r^2)$ operations, where k_{mt} and k_{mr} are the number of fine search grids in DOD and DOA, respectively. Generally, the computation burden of the AP based MLE algorithm is

heavier than the ESPRIT algorithm, since $2N_{iter}k_f$ is typically larger than N_tN_r for a moderate transmit and receive array. While for the MUSIC algorithm, it may need extremely fine 2D global search to obtain an accurate estimate of the target DOD and DOA. Thus, the computational complexity of the MUSIC algorithm may be higher than the AP based MLE algorithm.

7. Numerical simulation

In this section, we illustrate the MLE results of the target DOD and DOA with several numerical examples. The parameters used for simulation are listed as follows: the bistatic MIMO radar is equipped with $N_t=5$ transmitting antennas, and $N_r=5$ receiving antennas, both of which are ULAs with half-wavelength inter-element spacing. Moreover, the SNR in the simulations is defined by

$$\mathrm{SNR}=\frac{\sigma_s^2 N_t N_r}{\sigma^2}, \tag{34}$$

where σ_s^2 is the average power of the target signal.

In Fig. 2, the MLE results of the target DOD and DOA with $K=100$ i.i.d. samples and SNR = 10 dB over 50 Monte Carlo trials are presented. In this case, three uncorrelated targets are located in $(\theta_1,\phi_1)=(30^\circ,45^\circ)$, $(\theta_2,\phi_2)=(-8^\circ,30^\circ)$, $(\theta_3,\phi_3)=(0^\circ,5^\circ)$, respectively. In the initialization of the AP algorithm for the MLE of DOD and DOA of the target, the search space for the sine of every angle (defined as u-space in [21]) has an upper bound equal to 1 and a lower bound equal to -1 with the searching step size equal to 0.05 (or equivalently, $k_{ct}=k_{ct}=40$). During the iterations, we always partition the searching space into $k_f=1000$ uniform grids. The AP algorithm in this paper is terminated if the maximum variation of the angle estimation result is smaller than $\varepsilon=1\times10^{-8}$. And the constant w in the adapted searching space is 20. We can observe from Fig. 2 that the DOD and DOA of the three targets are correctly estimated.

In Fig. 3, a histogram showing the number of iterations required in the proposed AP algorithm is plotted for the 50 Monte Carlo trials conducted in Fig. 2. It is shown that

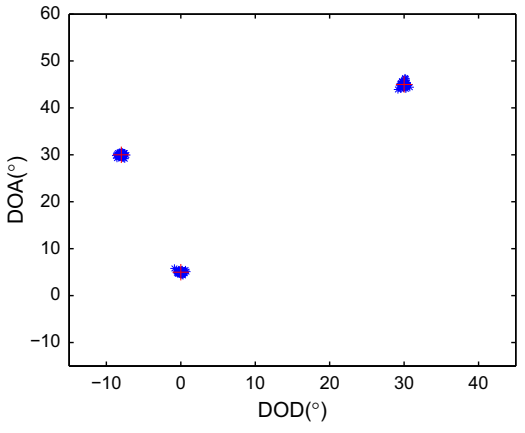

Fig. 2. Angle estimation results of the MLE: SNR=10 dB, $K=100$, 50 Monte Carlo trials.

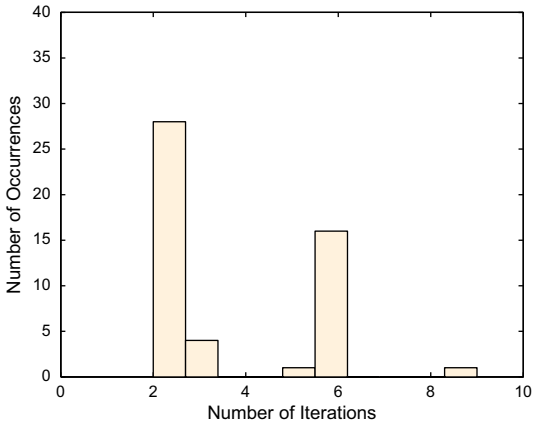

Fig. 3. Histograms of the number of iterations in the AP algorithms over the 50 Monte Carlo trials: SNR=10 dB, $K=100$.

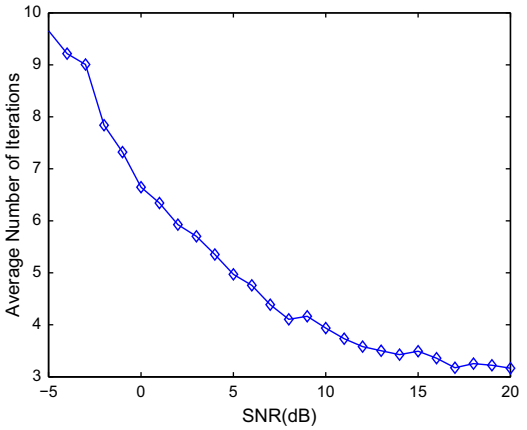

Fig. 4. Average number of iterations versus SNR: $K=100$.

the most common number of iterations in this case is 2. Thus the convergence rate of the AP algorithm is satisfactory.

Fig. 4 shows the average number of iterations with different SNR. The average number of iterations is obtained through 500 Monte Carlo trials with the same parameters as that in Fig. 2 while a changing SNR. We can observe from Fig. 4 that the average number of iterations required in the AP algorithm decreases with increasing SNR. This is because we can obtain a better initial estimate of the target DOD and DOA if the SNR is higher, and the improvement in the accuracy of the estimation result of DOD and DOA in the iterations is larger.

In Figs. 5 and 6, the mean square errors (MSE) of the MLE for the DOD and DOA of the first target are illustrated for different SNR, in which the number of samples $K=100$ and the other simulation parameters are the same as that in Fig. 2. Moreover, the MSE of the ESPRIT algorithm proposed in [12,13], the 2D MUSIC algorithm and the CRB given in Section 5 are plotted for comparison. It is shown that MSE of the MLE algorithm decreases with increasing SNR and it outperforms both the ESPRIT algorithm and the MUSIC algorithm, especially in the low SNR region. Furthermore, we can observe that the MLE algorithm and the MUSIC

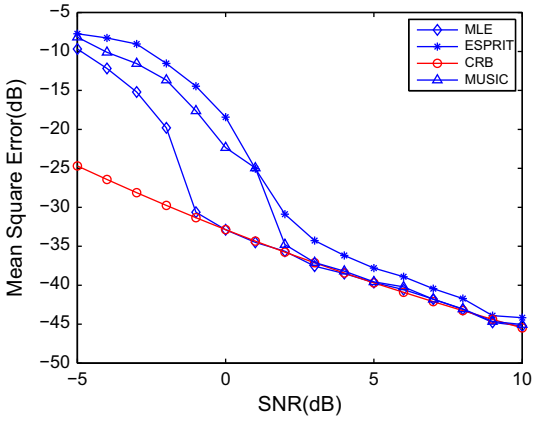

Fig. 5. CRB and mean square error (MSE) versus SNR for DOD of the first target: $K=100$.

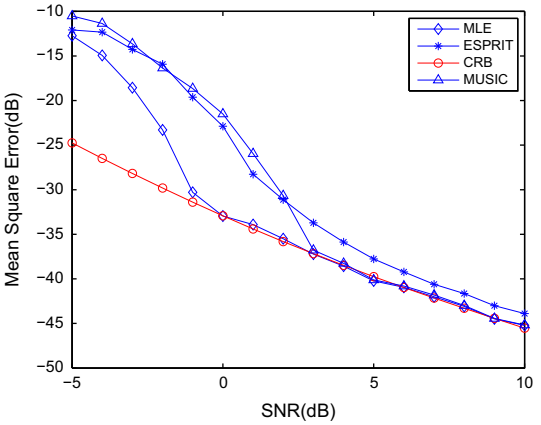

Fig. 6. CRB and mean square error (MSE) versus SNR for DOA of the first target: $K=100$.

algorithm can attain the CRB if the SNR is high. Nevertheless, the MLE algorithm can achieve the CRB with lower SNR (0 dB) than the MUSIC algorithm (3 dB).

Next we consider the performance of the MLE algorithm versus the number of samples when the target SNR is fixed. In this case, the target SNR is kept constant as 5 dB while the number of samples is varied with the other simulation parameters the same as that in Fig. 2. For brevity, we only present the MSE of the DOD and DOA of the second target in Figs. 7 and 8, respectively. It is shown in Figs. 7 and 8 that the performance enhancement of the MLE algorithm is clear with increasing number of samples. In addition, the MLE algorithm is superior to the ESPRIT and MUSIC algorithm and attains the CRB if K is larger than 30.

Now we further show the behavior of the three algorithms for the case in which the three targets are fully correlated. Here we use the same parameters as above with the targets being fully coherent. In Figs. 9 and 10, the MSE of the MLE, MUSIC and ESPRIT algorithm for the DOD and DOA of the third target is shown, respectively, in which $K=100$ and the target SNR is varied. We can observe from Figs. 9 and 10 that MLE algorithm works well in this case and it attains the CRB if the target SNR is

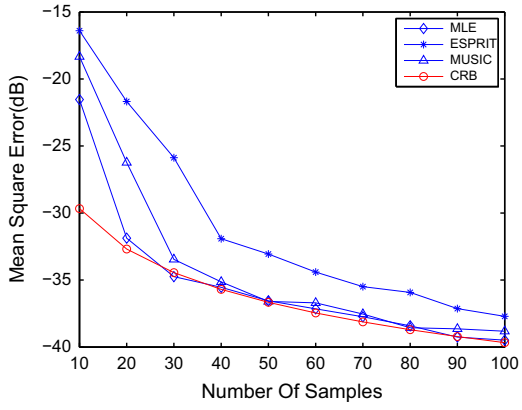

Fig. 7. CRB and mean square error (MSE) versus number of samples for DOD of the second target: SNR=5 dB.

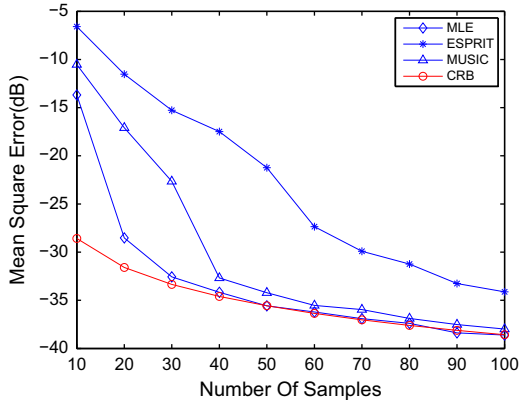

Fig. 8. CRB and mean square error (MSE) versus number of samples for DOA of the second target: SNR=5 dB.

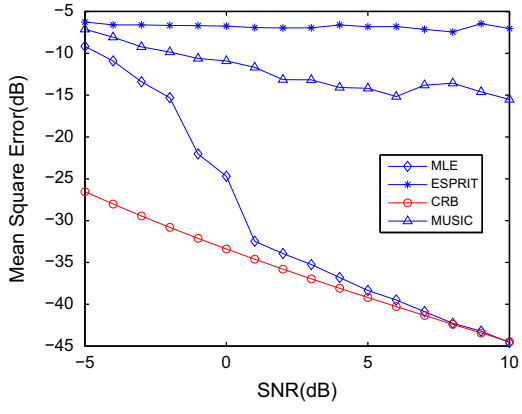

Fig. 9. CRB and mean square error (MSE) versus SNR for DOD of the third target: coherent targets and $K=100$.

relatively high. This can be explained by that MLE algorithm does not use the uncorrelated assumption of the target. Since the ESPRIT algorithm and MUSIC algorithm are derived based on that, the signal space is orthogonal to the noise space and the dimension of the signal space is

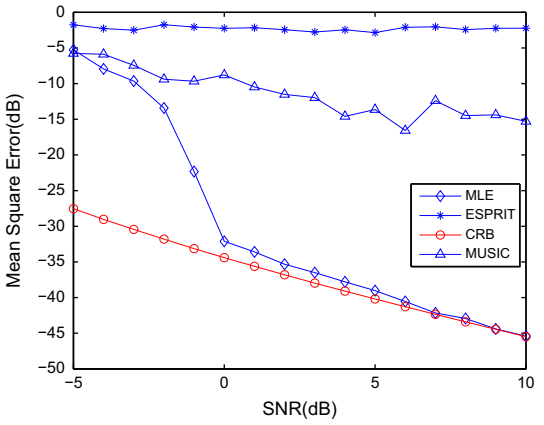

Fig. 10. CRB and mean square error (MSE) versus SNR for DOA of the third target: coherent targets and $K=100$.

equal to the number of targets, we can observe that they both fail in this circumstance.

8. Conclusion

In this paper, we have considered the problem of estimating the target DOD and DOA for bistatic MIMO radar with MLE. We have derived the maximum likelihood estimator of the target DOD and DOA based on the assumption that the targets are unknown but deterministic. Moreover, a compact expression for the CRB under this framework has been provided. In addition, we have proposed an AP algorithm which only needs 1D searches to reduce the computation load of solving the high-dimensional nonlinear optimization problem in finding the MLE of the targets. We have proved that the proposed AP algorithm converges locally and can converge to the global optimum in several iterations if a good initial point is given. Furthermore, the numerical results showed that the MLE algorithm behaved better than the ESPRIT and MUSIC algorithm for the uncorrelated target case and attained the CRB in the asymptotic region. For the case where the targets were fully coherent and the ESPRIT and MUSIC algorithm completely failed, the proposed MLE algorithm also worked quite well.

Acknowledgment

The authors would like to thank the editors and the anonymous reviewers for their helpful suggestions which lead to the improvement of this paper. This work was supported by the National Natural Science Foundation of China under Grant 61201379, and Anhui Provincial Natural Science Foundation under Grant 1208085QF103 The work of J. Tang was supported by the National Natural Science Foundation of China under Grant 61171120. The work of Y. Zhang was supported by the National Natural Science Foundation of China under Grant 61179036.

References

[1] J. Li, P. Stoica, MIMO radar with colocated antennas: review of some recent work, IEEE Signal Processing Magazine 24 (5) (2007) 106–114.
[2] A.H. Haimovich, R.S. Blum, L.J. Cimini, MIMO radar with widely separated antennas, IEEE Signal Processing Magazine 25 (1) (2008) 116–129.
[3] J. Li, P. Stoica, MIMO Radar Signal Processing, John Wiley & Sons, New Jersey, 2008.
[4] E. Fishler, A. Haimovich, R.S. Blum, L.J. Cimini Jr., D. Chizhik, R.A. Valenzuela, Spatial diversity in radars—models and detection performance, IEEE Transactions on Signal Processing 54 (3) (2006) 823–838.
[5] C.Y. Chen, P.P. Vaidyanathan, MIMO radar space time adaptive processing using prolate spheroidal wave functions, IEEE Transactions on Signal Processing 56 (2) (2008) 623–635.
[6] J. Li, P. Stoica, L. Xu, W. Roberts, On parameter identifiability of MIMO radar, IEEE Signal Processing Letters 14 (12) (2007) 968–971.
[7] N.H. Lehmann, E. Fishler, A.M.e. Haimovich, Evaluation of transmit diversity in MIMO-radar direction finding, IEEE Transactions on Signal Processing 55 (5) (2007) 2215–2225.
[8] Q. He, R.S. Blum, Diversity gain for MIMO Neyman–Pearson signal detection, IEEE Transactions on Signal Processing 59 (3) (2011) 869–881.
[9] N.H. Lehmann, A.M. Haimovich, R.S. Blum, L. Cimini, High resolution capabilities of MIMO radar, in: Fortieth Asilomar Conference on Signals, Systems and Computers (ACSSC '06), 2006, pp. 25–30.
[10] P. Stoica, J. Li, Y. Xie, On probing signal design for MIMO radar, IEEE Transactions on Signal Processing 55 (8) (2007) 4151–4161.
[11] H. Yan, J. Li, G. Liao, Multitarget identification and localization using bistatic MIMO radar systems, EURASIP Journal on Advances in Signal Processing 2008 (Article ID 283483) (2008) 1–8.
[12] D. Chen, B. Chen, G. Qin, Angle estimation using ESPRIT in MIMO radar, Electronics Letters 44 (12) (2008) 770–771.
[13] J. Chen, H. Gu, W. Su, Angle estimation using ESPRIT without pairing in MIMO radar, Electronics Letters 44 (24) (2008) 1422–1423.
[14] M. Jin, G. Liao, J. Li, Joint DOD and DOA estimation for bistatic MIMO radar, Signal Processing 89 (2) (2009) 244–251.
[15] M.L. Bencheikh, Y. Wang, H. He, Polynomial root finding technique for joint DOA DOD estimation in bistatic MIMO radar, Signal Processing 90 (2010) 2723–2730.
[16] J. Chen, H. Gu, W. Su, A new method for joint DOD and DOA estimation in bistatic MIMO radar, Signal Processing 90 (2) (2010) 714–718.
[17] R. Xie, Z. Liu, J. Wu, Direction finding with automatic pairing for bistatic MIMO radar, Signal Processing 92 (2012) 198–203.
[18] I. Bekkerman, J. Tabrikian, Target detection and localization using MIMO radars and sonars, IEEE Transactions on Signal Processing 54 (10) (2006) 3873–3883.
[19] N.J. Willis, Bistatic Radar, SciTech Publishing Inc., Raleigh, NC, 2005.
[20] X. Zhang, Z. Xu, L. Xu, D. Xu, Trilinear decomposition-based transmit angle and receive angle estimation for multiple-input multiple-output radar, IET Radar, Sonar & Navigation 5 (6) (2011) 626–631.
[21] H.L. Van Trees, Optimum Array Processing, John Wiley & Sons Inc., New York, 2002.
[22] P. Stoica, Y. Selén, Cyclic minimizers, majorization techniques, and the expectation–maximization algorithm: a refresher, IEEE Signal Processing Magazine 21 (1) (2004) 112–114.
[23] J.A. Tropp, I.S. Dhillon, R.W. Heath, Designing structured tight frames via an alternating projection method, IEEE Transactions on Information Theory 51 (1) (2005) 188–209.
[24] I. Ziskind, M. Wax, Maximum likelihood localization of multiple sources by alternate projection, IEEE Transactions on Signal Processing 36 (10) (1988) 1553–1560.
[25] P.J. Chung, J.F. Bohme, DOA estimation using fast EM and SAGE algorithms, Signal Processing 82 (2002) 1753–1762.